Strain of a biomembrane caused by a local tangential force: Application to magnetic tweezer measurements

A. A. Boulbitch*
Department of Biophysik E22, TU München, D-85747 Garching bei München, Germany
(Received 14 April 1998; revised manuscript received 20 July 1998)

Strain field in a cell membrane caused by application of a local force along its surface is studied theoretically. The cell cytoskeleton is assumed to give rise to a restoring force acting on the membrane. This contribution is shown to localize the membrane displacement. The results are used to discuss magnetic tweezers experiments on membranes of mouse fibroblasts.
[S1063-651X(99)05003-5]

PACS number(s): 87.10.+e, 87.19.Rr, 87.16.−b

Magnetic tweezers make it possible to study a viscoelastic behavior of biological materials. Since the paper of A. Heilbronn [1] this method was successfully applied to study the cytoplasmic viscosity [2], properties of a vitreous body [3], a mechanical response of a cell cytoskeleton to a twist applied to its surface [4]. It allowed to study activation of Ca^{2+} channels in fibroblasts [5], accumulation of *F*-actin at focal contacts [6], elasticity and motion of DNA molecules [7–9], and viscoelastic properties of actin solutions [10–12]. In the method described in the papers [11,12] a paramagnetic bead surrounded by nonmagnetic beads is embedded into a body. Application of inhomogeneous magnetic field **B** gives rise to a force $\mathbf{F}\sim\nabla(\mathbf{B})^2$ acting on the paramagnetic bead [11]. The latter can be treated as a source of a point force applied to a viscoelastic media, the nonmagnetic beads making it possible to study the displacement field in its several points. Application of this method to entangled [11] or cross-linked [12] three-dimensional actin networks showed a good agreement of the measured strain field with the elastic Green's function of the three-dimensional isotropic elastic media [12].

In contrast, the magnetic tweezers study of the membrane of mouse fibroblasts (Fig. 1) showed a contradictory result [13]. Membranes of animal cells consist of a lipid bilayer supported by actin cortex. The latter is attached to the bulk cell cytoskeleton. Paramagnetic beads coated by fibronectin are placed onto the membrane. Fibronectin provides a specific binding of the bead to the actin cortex of the membrane. Hence the force acting on the bead can be considered as that acting on the actin cortex. The radius of the magnetic bead is approximately 2.5 μm. However, the effective contact area in the place of attachment of bead-coating proteins to the membrane (referred to as ''a disk'') should be smaller. The size of the cell lobe (the flat part of the cell, Fig. 1) of the mouse fibroblast is about 10 μm. Thus the approximation of a localized force is reasonable.

We assume that membrane of a cell and, namely, its actin cortex has viscoelastic properties. There are several experimental observations supporting this assumption. First, microrheological and macrorheological experiments on three-dimensional (3D) entangled and cross-linked actin solutions [11,12,14] showed that these systems demonstrate a viscoelastic behavior characterized both by a shear modulus and viscosity. All the more, this kind of behavior should be expected in the actin cortex. Second, several direct measurements on cell membranes have shown a stress-strain dependence [4,13,15,16]. We interpret this as a manifestation of a visco-elastic behavior of studied systems. In this paper we focus mainly on an elastic part of the viscoelastic deformation of cell membranes in the magnetic tweezers measurements.

In a thin elastic plate to which a tangential force **F** is applied the displacement vector $\mathbf{u}=\mathbf{u}(\mathbf{r})$ obeys the equation of mechanical equilibrium,

$$\Delta\mathbf{u}+\frac{1+\sigma}{1-\sigma}\,\mathrm{grad}\,\mathrm{div}\,\mathbf{u}=-\mathbf{f}, \tag{1}$$

where **r** is the in-plane radius vector, $\mathbf{f}=2(1+\sigma)\mathbf{F}/Eh=\mathbf{F}/\mu h$; h is the plate height (in the case under consideration h is the height of the membrane); E is the Young's modulus of the plate material and σ is the Poisson ratio, $\mu=E/2(1+\sigma)$ is the shear modulus [17]. One can consider $\mu^*=\mu h$ as the membrane shear modulus. Note that Eq. (1) is valid for a thin elastic plate [17] and differs from that describing an elastic 3D body, in which the coefficient

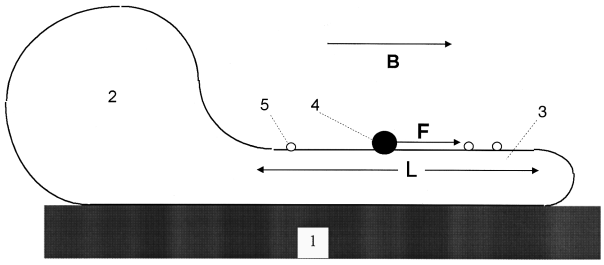

FIG. 1. Schematic view of application of the magnetic tweezers method to the case of the mouse fibroblast cell. 1, the substrate; 2, the cell; 3, the cell lobe; 4, the paramagnetic bead; and 5, the nonmagnetic bead attached to the cell membrane. Application of the magnetic field **B** causes the force **F** acting on the bead and hence on the membrane cortex. $L\sim 10\,\mu$m is the size of lobe.

*Address correspondence to Dept. für Biophysik E22, Technische Universität München, James Frank St., D-85747 Garching bei München, Germany. FAX: 49 (89) 2891-2469. Electronic address: aboulbit@physik.tu-muenchen.de

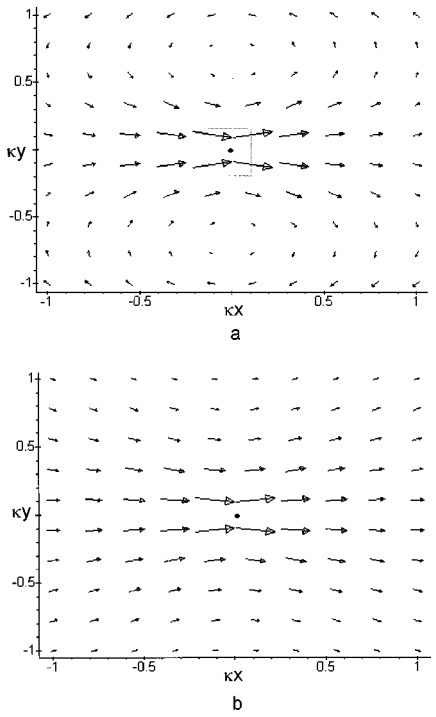

FIG. 2. The view of the displacement field $\mathbf{u}=(u_x,u_y)$ caused by the local force applied along $0x$ axis as the function of the dimensionless coordinates $(\kappa x,\kappa y)$. (a) The displacement field in the thin elastic plate described by Eq. (2). The cutoff distance is chosen to be $L=r_c=\kappa^{-1}$. (b) The displacement field in the membrane described by Eqs. (5) and (6). The Poisson ratio it taken to be $\sigma=0.5$. The dashed rectangle shows the region $r\ll r_c$ where equations of the conventional theory of thin plates (2) with $L=r_c$ approximate the complete Eqs. (5) and (6). The point shows the place, where the local force is applied.

$(1-2\sigma)^{-1}$ should be used instead of $(1+\sigma)/(1-\sigma)$ and one should omit h in the expression for $\mathbf{f}$ [18]. In the case of a thin infinite elastic plane to which the localized force $\mathbf{F}=\mathbf{F}_0\delta(\mathbf{r})$ is applied in the coordinate origin the expression for the displacement vector $\mathbf{u}=(u_x,u_y)$ has the form

$$u_x=-\frac{3-\sigma}{8\pi\mu^*}F_{0x}\ln\frac{r}{L}+\frac{1+\sigma}{16\pi\mu^*}\{F_{0x}\cos 2\theta+F_{0y}\sin 2\theta\},$$

$$u_y=-\frac{3-\sigma}{8\pi\mu^*}F_{0y}\ln\frac{r}{L}+\frac{1+\sigma}{16\pi\mu^*}\{F_{0x}\sin 2\theta-F_{0y}\cos 2\theta\}, \tag{2}$$

where F_{0x} and F_{0y} are the projections of the localized force, r and θ are the cylindrical coordinates of the radius vector. An arbitrary constant vector can be added to the solution Eq. (2) for the displacement vector, since it describes displacement of the whole plate as a solid body. This makes it possible to introduce an arbitrary parameter L with the dimension of a length (usually it is a plate size) [17]. Its value must be specified making use of conditions on the plate boundaries (or at infinity). The strain field $\mathbf{u}(x,y)=(u_x,u_y)$ describing by Eq. (2) caused by the force $\mathbf{F}=(F_0,0)$ applied along $0x$ axis is shown in Fig. 2(a). Thus in a thin plate the strain caused by the local force depends logarithmically on distance r from the observation point. In a finite plane this causes a strong influence of boundary conditions on the solution. In particular, the solution strongly depends on the mutual disposal of the point where the local force is applied and the plate boundaries. Some details and examples of exact solutions for thin plates to which local forces are applied one can find in Ref. [17]. Thus in the case of the elastic thin plate described by Eq. (1) and (2) the influence of the boundaries can in no case be considered as a small one.

However, results of the magnetic tweezers measurements on the membranes of mouse fibroblasts seem to contradict this picture. First, in a series of measurements an abrupt (possibly, exponential) decay of the displacement with distance from the magnetic bead was observed, while in another set of experiments the decay was observed to be more gentle. Second, observations show that the membrane displacement field caused by the magnetic bead placed in different parts of the membrane surface is very different, but up to now no indication was observed that it systematically depends on the distance of the magnetic bead from the boundary of the flat region [13] as should be expected from the conventional elastic theory [17].

This contradiction could be understood in taking into account the complex architecture of cell membranes. Animal cells usually exhibit a composite membrane consisting of a lipid bilayer, associated integral proteins, and an extracellular matrix. The bilayer is attached to a cellular cytoskeleton. The latter consists of a membrane coupled actin cortex, which is connected to the bulk cellular cytoskeleton [19]. Due to membrane complexity, the equation describing the its elastic response should differ from the simple equation of an elastic plate (1).

Note that one has already faced an analogous situation considering a normal force locally applied to a membrane [20]. If a local normal force is applied to a flat bilayer (or to a thin flat plate), the displacement of the bilayer is long range. Hence, boundary conditions play an important role independent of the lateral dimensions of the plate [18]. However, if a normal local force is applied to a cell membrane, the contribution of the cytoskeleton localizes its normal displacement, even if the membrane is flat [20]. This result enables us to expect that in the case of a force acting along the membrane surface the cytoskeleton may play a similar role.

In the present paper we propose to add to the equations of elastic equilibrium of a biomembrane a term describing the contribution of the cell cytoskeleton to the restoring force. We show that due to this contribution the membrane strain under application of a local tangential force is short range. In the light of these results we discuss the above contradictions in the magnetic tweezers experiments on the membrane of the mouse fibroblasts cell.

We assume that contribution of the cell bulk cytoskeleton gives rise to an additional restoring force acting on the actin cortex. The cytoskeleton consists of actin and intermediate filaments and microtubules and contains both extendable (elastic) and non-extendable elements. Both of them give rise to a restoring force proportional to the membrane displacement. Consider two naive mechanical models illustrating the origin of this restoring force (Fig. 3). In these models a thin elastic plate (representing the membrane) is attached to some rigid substrate either by springs [Fig. 3(a)], or by non-extendible filaments under tension [Figs. 3(b) and 3(c)].

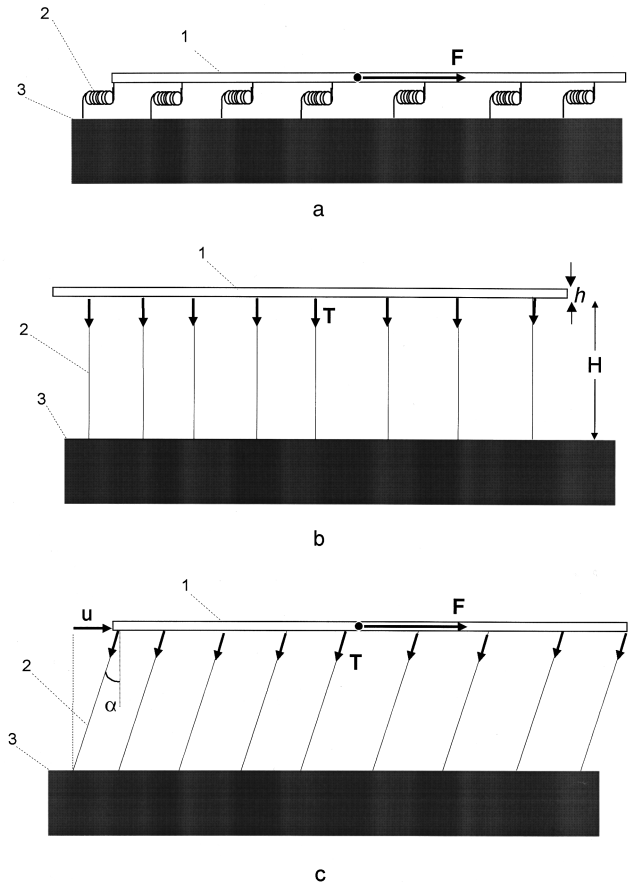

FIG. 3. Mechanical model illustrating arising of a restoring force in a membrane. (a) The plate (1) representing the membrane is attached to a substrate (3) by springs (2) with the total spring constant k and the restoring force $F_{\text{rest}}=ku$. (b) The plate (1) is attached to a substrate (3) by filaments (2), length H, which are under a constant tension $\mathbf{T}$. (c) A force $\mathbf{F}$ applied to the plate causes its shift $\mathbf{u}$, a tilt of filaments being $\alpha \approx u/H$ and a restoring force $F_{\text{rest}}=T\sin\alpha \approx Tu/H$. h is the membrane height.

These models reflect the fact that cell membrane is usually attached by its cytoskeleton to an immobilized cell part. The both models serve to show that there is a restoring force that acts on the plane from either the springs [Fig. 3(a)], or the filaments [Figs. 3(b) and 3(c)]. This force can be characterized by a spring constant.

To return from the simple mechanical models to the case of the cell membrane, one should add a restoring force $-\chi\mathbf{u}$ to the equations of equilibrium, where χ is a phenomenological spring constant density depending on elastic properties of the cytoskeleton. The equation of mechanical equilibrium takes the form:

$$\Delta\mathbf{u}+\frac{1+\sigma}{1-\sigma}\,\text{grad div}\,\mathbf{u}-\kappa^2\mathbf{u}=-\mathbf{f}, \tag{3}$$

where $\kappa^2=\chi/\mu^*>0$. In the case of the local force $\mathbf{F}=\mathbf{F}_0\delta(\mathbf{r})$ and correspondingly $\mathbf{f}=\mathbf{f}_0\delta(\mathbf{r})$. Making use of the Fourier transformation one gets

$$\mathbf{u}_\mathbf{q}=\frac{\mathbf{f}_0}{q^2+\kappa^2}-\frac{(1+\sigma)}{2}\,\frac{\mathbf{q}(\mathbf{q}\cdot\mathbf{f}_0)}{(q^2+\kappa^2)\left(q^2+\dfrac{1-\sigma}{2}\kappa^2\right)}, \tag{4}$$

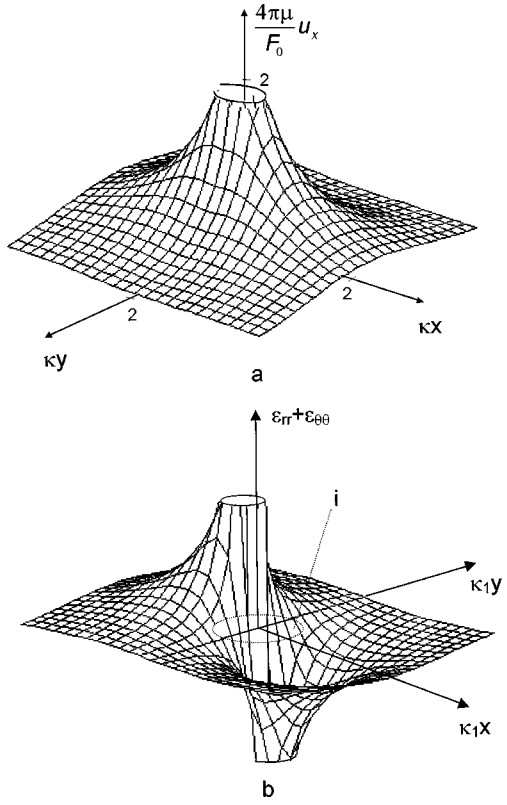

FIG. 4. Dependence of the component u_x (a) of the membrane in-plane displacement vector and of the trace of the strain tensor $\varepsilon_{\pi}+\varepsilon_{\theta\theta}$ on coordinates. (i) shows the position of the disk.

where $\mathbf{q}$ is the wave vector and $\mathbf{u}_\mathbf{q}$ is the Fourier transform of the displacement vector.

The inverse Fourier transformation yields the exact solution of Eq. (3):

$$u_x(\mathbf{r})=\frac{F_0}{2\pi\mu^*}\left\{\frac{1}{2}K_0(\kappa r)+\frac{1-\sigma}{4}K_0(\kappa_1 r)-\cos 2\theta\left[\frac{K_1(\kappa r)}{\kappa r}-\sqrt{\frac{1-\sigma}{2}}\,\frac{K_1(\kappa_1 r)}{\kappa r}+\frac{1}{2}K_0(\kappa r)-\frac{1-\sigma}{4}K_0(\kappa_1 r)\right]\right\}, \tag{5}$$

$$u_y(\mathbf{r})=-\frac{F_0\sin 2\theta}{2\pi\mu^*}\left\{\frac{K_1(\kappa r)}{\kappa r}-\sqrt{\frac{1-\sigma}{2}}\,\frac{K_1(\kappa_1 r)}{\kappa r}+\frac{1}{2}K_0(\kappa r)-\frac{1-\sigma}{4}K_0(\kappa_1 r)\right\}, \tag{6}$$

where K_0 and K_1 are the modified Bessel functions and $\kappa_1=[(1-\sigma)/2]^{1/2}\kappa$. We assumed here that the force $\mathbf{F}_0$ is applied along the $0x$ axis $\mathbf{F}_0=(F_0,0)$. Note that Eqs. (5) and (6) give the exact expression for the Green's function of the thin elastic plate supporting by an elastic substrate. The displacement field $\mathbf{u}(x,y)=(u_x,u_y)$ describing Eqs. (5) and (6) is shown in Fig. 2(b). Dependence of the component u_x of the displacement vector on coordinates is displayed in Fig. 4(a).

Rotation ω of the membrane elements is described by the relation $\omega=\partial u_x/\partial y-\partial u_y/\partial x$. Making use of the Fourier transform (4) one can find the explicit expression for the rotation caused by the local force $\mathbf{F}_0=(F_0,0)$:

$$\omega=-\frac{\kappa(1+\sigma)F_0}{\pi Eh}K_1(\kappa r)\sin\theta. \tag{7}$$

The rotation changes its sign on the $0x$ axis.

An especially simple form takes the combination $\varepsilon_{rr}+\varepsilon_{\theta\theta}$ of the components of the strain tensor ε_{ij} in the cylindrical coordinates,

$$\varepsilon_{rr}+\varepsilon_{\theta\theta}=-\frac{(1-\sigma)\kappa_1}{4\pi\mu^*}F_0\cos\theta K_1(\kappa_1 r), \tag{8}$$

that describes the two-dimensional stretching, or compressing of the membrane. Note that the membrane is free in the direction normal to its surface. Therefore, the in-plane membrane stretching is followed by its compression in the direction normal to the plane. Dependence of the trace of the strain tensor on coordinates is shown in Fig. 4(b).

The solution (5)–(8) is rather unwieldy. However, it contains a cutoff parameter with the dimension of length $r_c=\kappa^{-1}=[\mu^*/\chi]^{1/2}$, making it possible to consider short- and long-range regimes. In the short-range regime ($r\ll r_c$), making use of the expansions $K_0(\kappa r)\approx-\ln(\kappa r/2)-\gamma+\cdots$ and $K_1(\kappa r)\approx(\kappa r)^{-1}+\kappa r\{2\ln(\kappa r/2)+2\gamma-1\}/4+\cdots$ for the modified Bessel functions [21], (γ is the Euler constant) one returns to the solutions of the flat theory of elasticity, Eq. (2). As already noted above, in the conventional theory of thin plates conditions at the plate boundary must be taken into account when the local force is applied to the plate. In contrast, in the case under consideration if the size of the membrane is much larger than r_c one can use the solutions Eq. (2) as if the membrane were infinite and free at infinity. This simplification arises because displacements [Eqs. (5) and (6)] caused by the local force at the plate boundaries are negligible.

In the opposite regime $r\gg r_c$ (using the expression $K_n(\kappa r)\sim(\pi/2\kappa r)^{1/2}\exp(-\kappa r)$, $n=0,1$ [21] and keeping the most slowly vanishing terms in the solutions Eqs. (5) and (6)) one gets the asymptotics:

$$u_x\sim\frac{F_0(1-\sigma)\cos^2\theta}{4\mu^*(2\pi\kappa_1 r)^{1/2}}\exp(-\kappa_1 r);\quad u_y\sim u_x\tan\theta. \tag{9}$$

Thus the components of the displacement vector described by the model Eq. (3) increase logarithmically under $r\to0$ ($r\ll r_c$) and exponentially vanish at large distance ($r\gg r_c$).

The approximate expressions for the rotation in the two regimes take the form

$$\omega\approx\begin{cases}-\dfrac{(1+\sigma)F_0\sin\theta}{\pi Eh}\dfrac{1}{r}, & r\ll r_c\\[2ex] -\dfrac{\kappa^{1/2}(1+\sigma)F_0\sin\theta}{Eh(2\pi r)^{1/2}}\exp(-\kappa r), & r\gg r_c\end{cases}. \tag{10}$$

To discuss the results, consider the experimental geometry in more detail. One should distinguish two regions of the membrane. The first is the one attached to the magnetic bead. It is a disk, radius R (Fig. 5, region ii). The second region is the one outside the disk. Coating the bead with fibronectin is known to cause clustering of integrin molecules. It is the matter of general experience that such clustering gives rise to formation of stress fibers [22,23]. This is a reason to expect that actin filaments and bundles (Fig. 5(a), fragment *j*) should be formed in this region. They connect the disk (Fig. 5(a), fragment ii) either with the bulk cellular cytoskeleton, or with the bottom membrane. If $R\ll r_c$, one can consider the problem within the approximation of a local force. In this case a resulting local force $\mathbf{F}_0=(\mathbf{F}-\mathbf{F}_b)\delta(\mathbf{r})$ is applied to the membrane. Here $\mathbf{F}$ is the force applied to the disk from the part of the bead and $\mathbf{F}_b$ is the counterforce from the part of the filaments and bundles connected to the adhesion complexes within the disc (Fig. 5(a), fragment *j*). One finds $\mathbf{F}_b=-\pi R^2\chi_b\mathbf{u}_0$, where χ_b is the spring constant density related to the filaments and bundles and $\mathbf{u}_0$ is the displacement vector of the magnetic bead. One can obtain an approximate value of the magnetic bead displacement by averaging the displacement over the angle at $r=R$. With the help of Eqs. (5) and (6) one finds $\mathbf{u}_0=(u_{0x},0)$ with

$$u_{0x}=\frac{F-\pi R^2\chi_b u_{0x}}{4\pi\mu^*}\{K_0(\kappa R)+(1-\sigma)K_0(\kappa_1 R)\}. \tag{11}$$

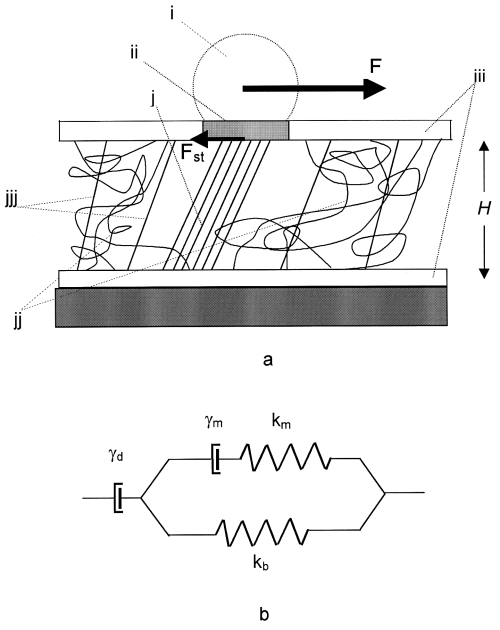

FIG. 5. (a) Schematic view of the model of the cell lobe with the magnetic bead attached to the top membrane. (i) the bead; (ii) the part of the membrane to which the bead is attached referred to as the disc; (iii) the top and the bottom membranes; (j) the actin bundles caused by the attachment of the bead; (jj) the unstressed and (jjj) the stressed parts of the cytoskeleton. (b) The equivalent mechanical circuit. The dashpot with the effective coefficient of viscous friction γ_d is attributed to the viscous motion of the bead relative to the membrane in the disk region; the dashpot γ_m and the spring with the constant k_m describe the viscoelastic behavior of the membrane; the spring k_b describes the contribution of the filaments and bundles attached to the disk.

Making use of Eq. (11) one obtains the force-displacement relation

$$\mathbf{F}=-(g\mu^*+\pi R^2\chi_b)\mathbf{u}_0, \tag{12}$$

where g is the dimensionless geometric factor: $g=4\pi\{K_0(\kappa R)+(1-\sigma)K_0(\kappa_1 R)\}^{-1}$ One can consider the parameter $k=g\mu^*+\pi R^2\chi_b$ as an effective spring constant of the system.

So far, we have considered the elastic behavior of the system. Now we discuss briefly its viscous behavior. One should expect two kinds of viscous motion in the system. The first of them is related to the viscous flow of the actin cortex outside of the disk. It can be characterized by its viscosity η_m. Due to its contribution the equation of motion of the bead contains a term describing a viscous friction. It is characterized by an effective coefficient of viscous friction γ_m with $\gamma_m\sim\eta_m$.

The second is related to the viscous behavior of the disc itself [region ii, Fig. 5(a)]. Consider the strain tensor ε_{ij} in the vicinity of the disc boundary. If $R\ll r_c$, one finds

$$\varepsilon_{rr}+\varepsilon_{\theta\theta}\approx-\frac{(1-\sigma)F}{4\pi\mu^*}\frac{\cos\theta}{R};$$

$$\varepsilon_{rr}-\varepsilon_{\theta\theta}\approx-\frac{F}{2\pi\mu^*}\frac{\cos\theta}{R};\quad 2\varepsilon_{r\theta}\approx\frac{(1-\sigma)F}{4\pi\mu^*}\frac{\sin\theta}{R}. \tag{13}$$

One can see that the value $\varepsilon_{rr}+\varepsilon_{\theta\theta}$, Eq. (13), is negative at $-\pi<\theta<\pi$. This corresponds to the in-plane tensile strain that takes its maximum value at $\theta=0$, $r=R$, i.e., in front of the disk [Fig. 4(b)]. The high value of the tensile strain, Eq. (13), and of the corresponding stress, should give rise to a manifested plastic behavior in the vicinity of a point $\theta=0$, $r=R$. Analogous dependence is demonstrated by the combination $\varepsilon_{rr}-\varepsilon_{\theta\theta}$ of components of the strain tensor, describing an in-plane biaxial tension that also takes its extremum value at $\theta=0$, $r=R$. In contrast, the shear component of the strain tensor $\varepsilon_{r\theta}$ takes its extremum values at $r=R$, $\theta=\pm\pi/2$. Therefore, since the plastic flow anyway takes place in the actin cortex, it will be maximum at the points of the disk boundary $r=R$; $\theta=0$ and $\theta=\pm\pi/2$. However, the molecular structure of the membrane in the disc is different from that of the outside membrane. Hence, the viscosity of the disk η_d is different from η_m. The viscosity of the disk gives rise to a viscous friction term in the equation of motion of the bead characterized by an effective coefficient of viscous friction γ_d. The latter describes the viscous friction during the bead motion relative to the membrane.

One can, therefore, describe the system in terms of an equivalent mechanical circuit with a Kelvin-Zener circuit and a dashpot γ_d in series [Fig. 5(b)]. One of the two springs of the Kelvin-Zener circuit with the spring constant $k_b=\pi R^2\chi_b$ describes the elastic contribution of actin filaments and bundles attached to the disk, and the other one with the spring constant $k_m=g\mu^*$ accounts for the elastic contribution of the membrane. It is in series with the dashpot γ_m.

Discuss in more details the nature of the restoring force. In the present approach, the cell membrane consisting of the lipid bilayer attached to the actin cortex is represented by a thin viscoelastic plate supported by an elastic substrate. Magnetic tweezers measurements are made on a cell lobe (Fig. 1). The lobe shape makes it possible to assume that its top membrane is flat. The bottom membrane can be considered as rigid and fixed to the solid substrate. A basic assumption of the present model is that the actin cortex is coupled to the bulk cytoskeleton. The latter consists of microtubules, intermediate filaments and actin filaments. The bulk cytoskeleton may consist of unstressed and prestressed compartments. The unstressed parts of the cytoskeleton can be characterized by the number density $n_{\rm un}$ of attachments of these components to the actin cortex and by an average spring constant $k_{\rm un}$. They are shown schematically in Fig. 5(a) [cf. Fig. 3(a)]. The prestressed parts of the cytoskeleton consist of filaments and bundles under tension. They may either penetrate the whole thickness of the lobe connecting the top and the bottom membranes, or connect the top membrane to a stressed region of the network, that is attached to the bottom membrane by another filament. Assume that the lobe possesses $n_{\rm st}$ such filaments per unit area and that they exhibit an average tension T [cf. Figs. 3(b) and 3(c)]. An in-plane displacement of the cortex $\mathbf{u}=(u_x,u_y)$ is followed by tilting of the stress fibers in the prestressed parts of the cytoskeleton. It causes bending of the stiff microtubules and intermediate filaments and stretching of wrinkles and meshes of the unstressed parts of the cytoskeleton. Under a lateral membrane displacement $\mathbf{u}$ both mechanisms give rise to a restoring force $|\mathbf{F}_{\rm rest}|=S(Tn_{\rm st}\tan\alpha+k_{\rm un}n_{\rm un}|\mathbf{u}|)$, where S is the membrane area, α being the tilt angle [Fig. 3(c)]. The first term describes the contribution of the prestressed and the second one that of the unstressed cytoskeletal components. Making use of the relation $\tan\alpha\approx u/H$ one finds $\mathbf{F}_{\rm rest}=-S(Tn_{\rm st}/H+k_{\rm un}n_{\rm un})\mathbf{u}$. Here H is the distance between the top and the bottom membranes of the cell lobe [Figs. 3(b), and 5(a)]. One defines the coupling constant χ as $\mathbf{F}_{\rm rest}=-S\chi\mathbf{u}$, whence it follows $\chi=k_{\rm un}n_{\rm un}+Tn_{\rm st}H$. Thus, one obtains

$$r_c=\left(\frac{\mu^*H}{k_{\rm un}n_{\rm un}H+Tn_{\rm st}}\right)^{1/2}. \tag{14}$$

In the case of a thin lobe ($H\ll Tn_{\rm st}/k_{\rm un}n_{\rm un}$) one finds $r_c\approx(H\mu^*/Tn_{\rm st})^{1/2}$. In this limit the cutoff radius is determined by the tension of the stress fibers. In the opposite case one gets the cutoff radius depending on the unstressed parts of the cytoskeleton $r_c\approx(\mu^*/k_{\rm un}n_{\rm un})^{1/2}$. In a real cell the mechanism of formation of the restoring force can be more complicated. Therefore, one should consider the coupling constant χ as a phenomenological parameter.

We show that the restoring force caused by the cytoskeleton should be taken into account in equations of equilibrium of the cell membrane. Assuming that the membrane is homogeneous, this contribution is described by the phenomenological parameter—the cutoff distance $r_c=\kappa^{-1}$. It makes the displacement caused by a local tangential force to be localized within the region the size of which is of the order of the magnitude of r_c. The experimental results [13] give an estimation of the cutoff distance of approximately a few micrometers. An analogous result was obtained earlier in the case of a local force applied normally to the cell surface. In the latter case this was the effect of contributions both of the

bulk cellular cytoskeleton and the rigidity of the curved cellular membrane [20]. Therefore, it is established that the local force applied under an arbitrary angle to the cell surface causes its localized displacement within a cutoff distance. This result is in agreement with the observations of Glogauer *et al.* [6]. In their work the local force was applied normally to the surface of a stromal cell. The observations were interpreted in terms of a model suggesting that application of a normal force is followed by opening of Ca++ channels within a distance determined by some threshold tension. On the basis of the results of the present paper, one can see that this distance is somewhat smaller than the cutoff radius. Glogauer *et al.* observed that the influx of Ca++ was accompanied by an accumulation of actin in the vicinity of the disk [6]. This gradually increases the rigidity of the cytoskeleton and the coupling constant χ. Our results show that in this case the cutoff radius gradually decreases. This should reduce the number of channels opened, and gradually stop the actin accumulation, in correspondence with the observation of the paper [6].

The description of the membrane strain with the constant value of r_c is related to the assumption that the actin cortex and the adjacent part of the bulk cytoskeleton are homogeneous along the cell surface, which is not the case in real cells. The actin cortex and the bulk cytoskeleton are highly dynamic structures, and a number of effects cause inhomogeneities in the membrane. For example, depolymerization of cortical actin, a decrease in cross linking of actin filaments or even a rupture of the cortex can locally reduce the elasticity of the cortex or density of the bulk cytoskeleton adjacent to the membrane. If the scale on which the membrane significantly changes its properties is larger than r_c, the above approach is valid. In this case if in some region the spring constant density χ is small and the Young's modulus is large, the cutoff distance r_c may be relatively large and the membrane behaves like a conventional thin elastic plane. In contrast, in the regions with a small value of E and a large χ, the cutoff radius may be rather small. In particular, it can become as small as the size of the paramagnetic bead. In this case displacements of the nonmagnetic beads can be hardly observed. These considerations can explain the above-mentioned experimental observations [13], which previously seemed to be self-contradictory.

In this paper we propose that, except the strain, no other internal degree of freedom of the membrane remarkably influences its in-plane displacement. At the present time experimental results are not enough to find out to what extent this assumption is correct—its clarification requires further investigations.

I am grateful to E. Sackmann, whose discussions stimulated this work. This work was partially supported by the Alexander von Humboldt Foundation and by the Deutsche Forschungsgemeinschaft under Grant No. SA 246/28-1.

[1] A. Heilbronn, Jahrb. Wiss. Bot. **61**, 284 (1922).
[2] M. Sato, T. Z. Wong, D. T. Brown, and R. D. Allen, Cell Motil. Cytoskeleton **4**, 7 (1984).
[3] B. Lee, M. Litt, and G. Buchsbaum, Biorheology **29**, 521 (1992).
[4] N. Wang, J. P. Butler, and D. E. Ingber, Science **260**, 1124 (1993).
[5] M. Glogauer, J. Ferrier, and C. A. G. McCulloch, Am. J. Physiol. **269**, C1093 (1995).
[6] M. Glogauer, P. Arora, G. Yao, I. Sokolov, J. Ferrier, and C. A. G. McCulloch, J. Cell. Sci. **110**, 11 (1997).
[7] S. B. Smith, L. Finzi, and C. Bustamante, Science **258**, 1122 (1992).
[8] T. R. Strick, J.-F. Allemand, D. Bensimon, A. Bensimon, and V. Croquette, Science **271**, 1835 (1996).
[9] M. J. E. Richardson and G. M. Schuetz, Physica A **235**, 440 (1997).
[10] K. S. Zaner and P. A. Valberg, J. Cell Biol. **109**, 2233 (1989).
[11] F. Ziemann, J. Rädler, and E. Sackmann, Biophys. J. **66**, 2210 (1994).
[12] F. G. Schmidt, F. Ziemann, and E. Sackmann, Eur. Biophys. J. Lett. **24**, 348 (1996).
[13] F. G. Schmidt, A. R. Bausch, F. Ziemann, and E. Sackmann (unpublished); A. R. Bausch, F. Ziemann, A. A. Boulbitch, K. Jacobson and E. Sackmann, Biophys. J. **75**, 2038 (1998).
[14] B. Hinner, M. Tempel, E. Sackmann, K. Kroy, and E. Frey, Phys. Rev. Lett. **81**, 2614 (1998).
[15] N. Wang and D. Ingber, Biophys. J. **66**, 2181 (1994).
[16] B. Fabry, G. N. Maksym, R. D. Hubmayr, J. P. Butler, and J. J. Fredberg, J. Magn. Magn. Mater. (to be published).
[17] N. I. Muschelisvili, *Some Basic Problems of the Mathematical Theory of Elasticity* (Gronigen, Noordoff, 1963).
[18] L. D. Landau and E. M. Lifshitz, *Theory of Elasticity* (Pergamon, New York, 1959).
[19] E. Sackmann, in *Structure and Dynamics of Membranes, From Cells to Vesicles*, edited by R. Lipowsky and E. Sackmann (North-Holland, Amsterdam, 1995), Vol. 1A, pp. 1–63.
[20] A. A. Boulbitch, Phys. Rev. E **57**, 2123 (1998).
[21] *Handbook of Mathematical Functions*, edited by M. Abramowitz, and I. A. Stegun (Dover, New York, 1970).
[22] S. Miyamoto, S. K. Akiyama, and K. M. Yamada, Science **267**, 883 (1995).
[23] M. E. Chicurel, R. H. Singer, C. J. Meyer, and D. E. Ingber, Nature (London) **392**, 730 (1998).